Available online at www.sciencedirect.com
ScienceDirect
Trans. Nonferrous Met. Soc. China 25(2015) 2018−2026
Transactions of Nonferrous Metals Society of China
www.tnmsc.cn

Effect of gelcasting conditions on quality of porous Al−Cu alloy

Hai-ying YUAN, Cheng-chang JIA, Cong-cong WANG, Yu-hong CHANG,
Xin-xin ZHANG, Bekouche KARIMA, Zhao-li WANG

School of Materials Science and Engineering, University of Science and Technology Beijing, Beijing 100083, China

Received 28 July 2014; accepted 14 November 2014

Abstract: The porous Al−Cu alloy was prepared by the gelcasting process. And the effects of gelcasting conditions, such as monomer, the volume ratio of cross-linker and monomer, dispersant and redox initiating system on the height, gelling time and the quality of green body were investigated. (It was found that the dispersant and monomer played significant roles in the height and quality of green bodies, respectively.) The optimal conditions were 10% monomer, 2% cross-linker, 0.2% initiator (volume fraction), and 1.2 g dispersant, in which the green body exhibited the best quality. The mechanisms of process conditions in eliminating the cracks and forming the pores of in the five stages were proposed. Mercury porosimetry provided a description of pore diameter ranging from 10 to 10000 nm and open porosity of 38.78 %.

Key words: porous Al−Cu alloy; non-aqueous gelcasting; process conditions; crack; pore

1 Introduction

Aluminum−copper alloy has high temperature plasticity, machinability, good heat treatment in a cold hot pressure processing, and good ductility after annealing and quenching [1]. Up to now, there are several technologies, like laser surface melting [2], squeeze casting [3], steady-state solidification [4] and powder metallurgy [5] known for the manufacturing of aluminum−copper alloy with relatively different performances. However, there are few researches on the process of gelcasting.

As a novel in-situ colloidal forming technology with the advantage of low-cost machining, rapid production of large size, high reliability and complex shape, gelcasting is widely used in the fields of ceramic and metal parts [6−9]. The evaporation of solvent and the pyrolysis of organic polymer leave micro-pores and macro-pores in the green body. And the addition of foaming agents enhances the pore porosity [10]. So, it is widely used in the dense and porous material parts.

However, in this coagulation method, defects such as bubbles, delamination, micro-cracks, stresses, uneven distribution of concentration inside the body cause cracks in the sintered body, resulting in bad performance [11]. The cracks in the green bodies are usually generated in the solidification of suspension from liquid to gel, solvent removal, binder removal or sintering stage. This phenomenon is not only limited to the surface of the body, but also inside especially for large-shape samples during drying and degreasing processes. The inner stresses in green bodies are caused by the gradient of initiator concentration and temperature distribution in the forming stage, the gradient of temperature and humidity in the drying stage, and the narrow temperature range in the burning out stage [12]. The reason for inner stresses and random cracks is the non-uniform shrinkage caused by the uneven distribution of the components and density. The inner stress in the green body is induced by small amount of monomers [13], copolymerization of hydroxyl-ethyl-acrylate and acrylamide or addition of proper polyethylene glycol [11], the liquid desiccant PEG 1 000 on the drying process [14], and pure calcium aluminate cement [15]. Most of the studies have been therefore focused on the field of ceramics materials, and few attempts have been carried out with the aim of eliminating cracks in metal green body especially aluminum−copper alloys via adjusting process conditions.

Optimal gel formulation has a great difference for the same powder particles due to different gelcasting

Foundation item: Project (51274041) supported by the National Natural Science Foundation of China
Corresponding author: Cheng-chang JIA; Tel: +86-13691599749; E-mail: jiachc@126.com
DOI: 10.1016/S1003-6326(15)63811-0

systems, which gives rise to cracks in green bodies to different degrees. In order to eliminate the cracks in the green body and sintered body of aluminum−copper alloys by non-aqueous gelcasting systems, the effects of monomer, cross-linker, initiator and dispersant on the height, gelling time and quality of green body were investigated. The reason that causes cracks in different stages was also studied and the optimal formulation for aluminum−copper alloy was proposed.

2 Experimental

2.1 Materials

Spherical aluminum powder (purity> 99.97%) and spherical copper powder were used. Aluminum powder (purity >99.8%) with a mean particle size of 27.125 μm, specific surface of 0.279 m^2/cm^3 and particle size distribution ranging from 9.95 μm to 54.64 μm produced by Henan Yuanyang Aluminum Industry Co., Ltd., China was used. Copper powder with a mean particle size of 22.546 μm, specific surface of 0.366 m^2/cm^3 and particle size distribution ranged from 5.97 μm to 64.79 μm produced by Xingrongyuan Co., Ltd., China, was used as starting materials for non-aqueous gelcasting.

Table 1 shows the chemical reagents for non-aqueous gelcasting systems. Catalyst and initiator were the redox initiating system. All reagents were of analytically grade and were used as received without further purification.

Table 1 Chemical reagents for non-aqueous gelcasting systems

Monomer	Solvent	Cross-linker	Dispersant	Catalyst	Initiator
HEMA	PBO	DEGDA	PVP	DMA	CHP

2.2 Experimental procedure and characterization

Monomer, solvent, cross-linker and dispersant were mixed in a certain proportion to prepare a homogeneous slurry. The slurry was stirred on a magnetic machine after adding mixed metal powders slowly to ensure that the powders were completely wetted by the slurry. Before casting into the mold, the catalyst and initiator were added and stirred to prevent concentration gradient. The homogeneous suspension was slowly cast into the organic glass mold (d18.89 mm × 19.00 mm) at 60 °C with the glass rod. In-situ polymerization of the suspension occurred after 60 min, and the green bodies with high strength were demoulded. The green bodies were dried in the vacuum oven at 60 °C for 4 h and at 170 °C for 2 h. Then, the green bodies were burned out and sintered in the sintering furnace.

Gelling time of suspension from liquid to gel was measured with a stopwatch. All the experiments were carried out in triplicate, and the errors were controlled within 0.4%. Body height after demoulding was measured with a vernier caliper. The quality of green bodies was monitored during the five stages: solidifying, drying at 60 °C, drying at 170 °C, burning out and sintering.

The body quality was judged by the system of scoring: in the forming stage, the sample without the formation of gel was defined as 0, the green body with very weak strength which cannot be demoulded successfully was defined as 0.5, the green body with a large number of gels on the surface was defined as 1, and the green body with a small amount of gels or without gel on the surface was defined as 2; in the low temperature drying stage, the green body without cracks was defined as 3, then the cracks were divided into three levels according to the amount of cracks, respectively 0, 1 and 2; in the high temperature drying stage, the green body without cracks was defined as 4, then the green body with cracks both around and on the surface was defined as 0, the green body with cracks either around or on the surface was defined as 1 and 2 according to the amount of cracks; in the two stages of burning out and sintering, the system was the same, no crack was 0.5, and with crack was 0. The final scores were obtained by adding the scores in the every stage.

Fracture and surfaces were examined using scanning electron microscope (SEM, JSS 6510, Japan). The phase formation of polished sample was carried out by X-ray diffraction with Cu K_α radiation (XRD, TTR III system, Japan). The density, porosity, pore size distribution, cumulative pore volume and area were determined by mercury porosimetry (AutoPore IV 9500, USA).

3 Results and discussion

3.1 Effect of process conditions on body height

The effects of process conditions on the body height are shown in Fig. 1. As seen from Fig. 1, when adding 5% monomers corresponding to the ratio between cross-linker and monomer of 0.1, the gel cannot be formed successfully within the valid time, so that the body height is zero. This has a great influence on the formation of gel. Other data show small fluctuations and the difference between the maximum and minimum value is within 10 mm. Figures 1(a)−(c) show that the height of the green body increases gradually with the concentration of monomer, cross-linker and initiator. The increasing organics leads to more polymers per unit area, promoting the formation of more long-chain polymers and the increase of the height. The powder particles are firmly wrapped by long-chain polymers, making particle distribution in the body more uniform and improving the stability significantly. However, when volume fraction of

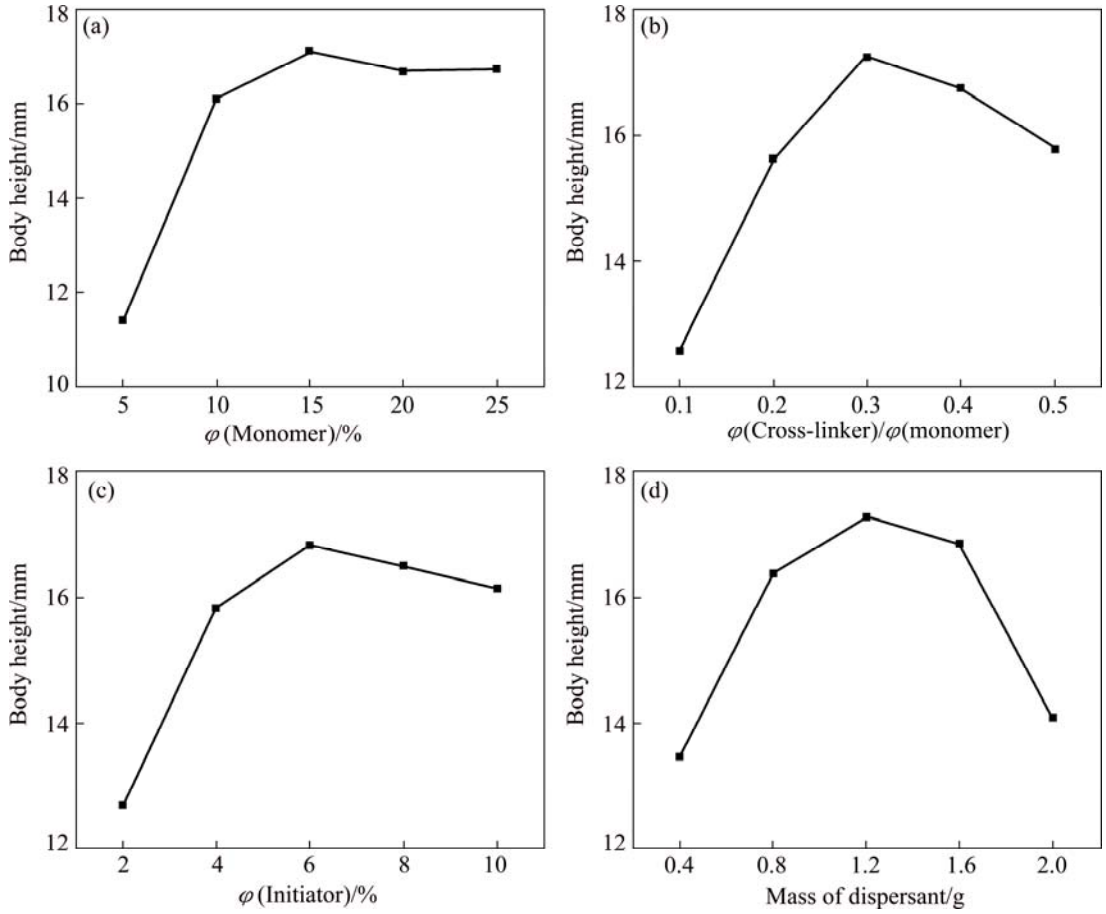

Fig. 1 Influence of process conditions on body height: (a) Monomer content; (b) Cross-linker/monomer ratio; (c) Initiator content; (d) Mass of dispersant

the monomer, the ratio of cross-linker and monomer, and volume fraction of initiator reach 15%, 0.3, 6%, respectively, as shown in Figs. 1(a)−(c), polymers around the powders are oversaturated, resulting in the height almost unchanged. Thus, there are some suspensions on the top of green bodies, lowering the height of green bodies.

Figure 1(d) shows that the concentration of dispersant has a remarkable effect on the height. Polyvinylpyrrolidone is a non-ionic and water-soluble polymer, showing the nature of anionic surfactant. The dispersant is easily dissolved in the solvent of 1, 2-propanediol not only due to the solvation energy and steric hindrance effect of the adsorption layer preventing powder particles from agglomerating, but also due to the strong bonding ability adsorbing easily on the surface of the colloidal particles to protect the colloid [16]. Nevertheless, when the concentration of dispersant is too low, the capability of steric hindrance is not strong enough to effectively adsorb particles on the surface resulting from small repulsive force between the particles. Similarly, when the concentration is too high, the particles are bridged by the excessive polymer chain, thus the excessive polymer chain limit mutual movement between particles that tend to coagulation [17]. Hence, both unsaturated adsorption and oversaturated adsorption prevent particles from dispersing in the solvent. The appropriate dispersant mass of 1.2 g enables the dispersant to exhibit the best stability and maximum height of green body.

3.2 Effect of process conditions on gelling time

The concentration of organics in per unit area between the powder particles is reduced with small amounts of the chemical reagents. When adding other organic compounds, the contact distance of two organics increases, then the reaction rate is reduced and gelling time is extended, as shown in Fig. 2. But the data clearly indicate that the polymerization is not accelerated obviously by the increase of monomer, cross-linker and initiator. When the volume fractions of monomer, the ratio of cross-linker and monomer, the volume fraction of initiator and the mass of dispersant reach 10%, 0.4, 4%, 1.6 g, respectively, and the gelling time can be shorten.

As shown in Fig. 2(a), the reaction probability of combining initiating radicals with monomer rises with the monomer content, and monomer will react with

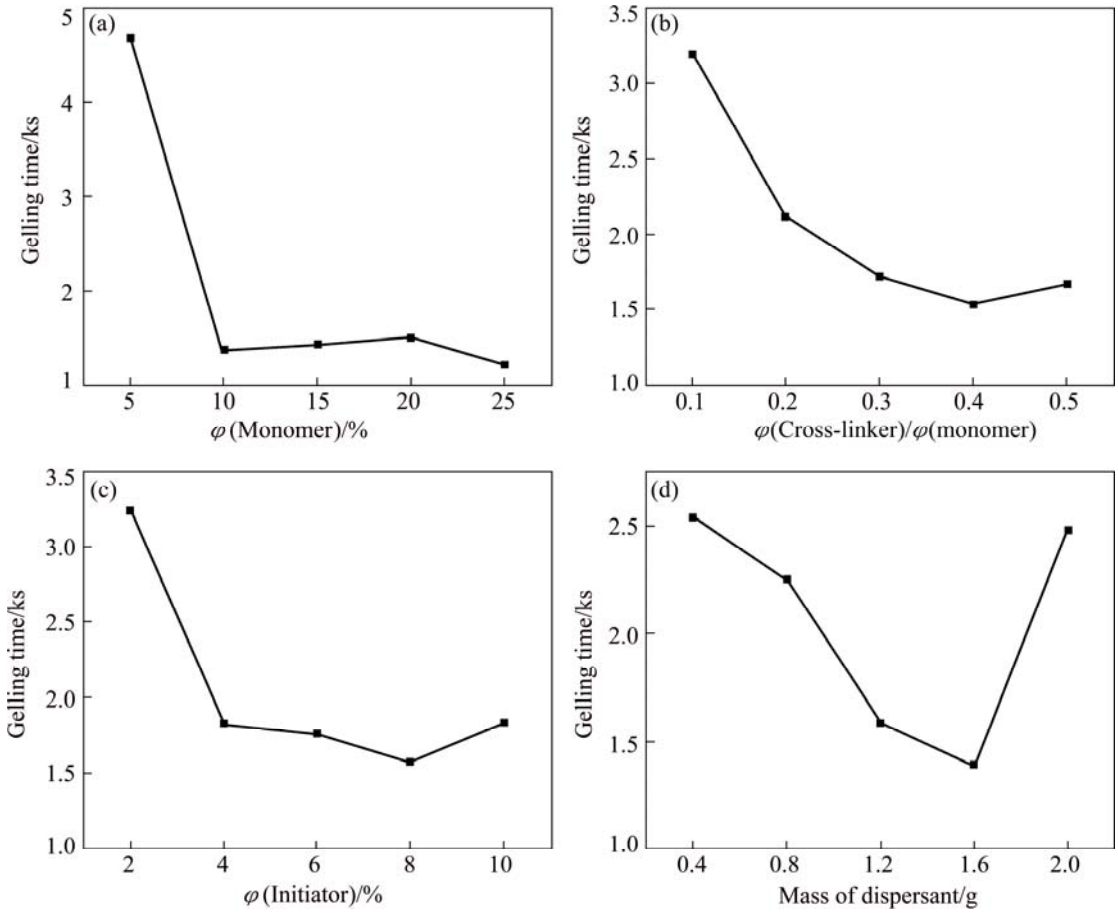

Fig. 2 Influence of process conditions on gelling time: (a) Monomer content; (b) Cross-linker/monomer ratio; (c) Initiator content; (d) Mass of dispersant

inhibiting substances such as oxygen or impurities in the slurry. Once inhibiting substances disappear, induction period is shortened, and gelation process is accelerated [18]. The initiation of monomers is determined by activation energy, and the energy in the suspension is fluctuating, exhibiting a linear distribution, so the initiation is affected by complex factors [19].

As shown in Fig. 2(c), free radicals created by initiator continuously will combine monomer molecules in the short time, promoting initiator efficiency and polymerization of the monomers. But the probability of collisions between free radicals increases with more initiators, resulting in the chain termination, at the same time, the loss of some free radicals is impacted by induced decomposition, cage effect or other side reactions, thereby reduce the reaction speed [18].

The steric hindrance effect of dispersant plays a significant role in the uniform distribution of particles around the organics of the suspension. The increase of dispersant mass makes more powder particles wrapped up in the organics when solidified, and reducing the reaction time, but when adding 2.0 g dispersant, there will be coagulation phenomenon, extending the gelling time, as shown in Fig. 2(d).

3.3 Effect of process conditions on body quality

The monomer constitutes a major component of cross-linked polymer gels. The content of monomers determines the length of molecular chains and the polymer network structures in the forming stage.

Figure 3(a) shows that 5% organic monomers cause lower strength of green bodies, so that they cannot be successfully demoulded in the effective time, making the quality of the body in the forming stage decrease significantly. The increase of the organic monomer will generate excessive monomer radicals. It not only promotes the reaction of polymerization, but also increases the gel network structures, thereby green bodies with enough strength can be successfully demoulded. However, more monomer molecules produce higher relative molecular mass polymer and longer polymer chains, which generate more inner stress. Inner stress generates, develops and inherits continuously in the drying stage, and inner stress within the body exceeds the maximum stress that the body can stand, resulting in the release of stress in the green body and the appearance of the cracks, so the quality of body decreases after the process of drying [13].

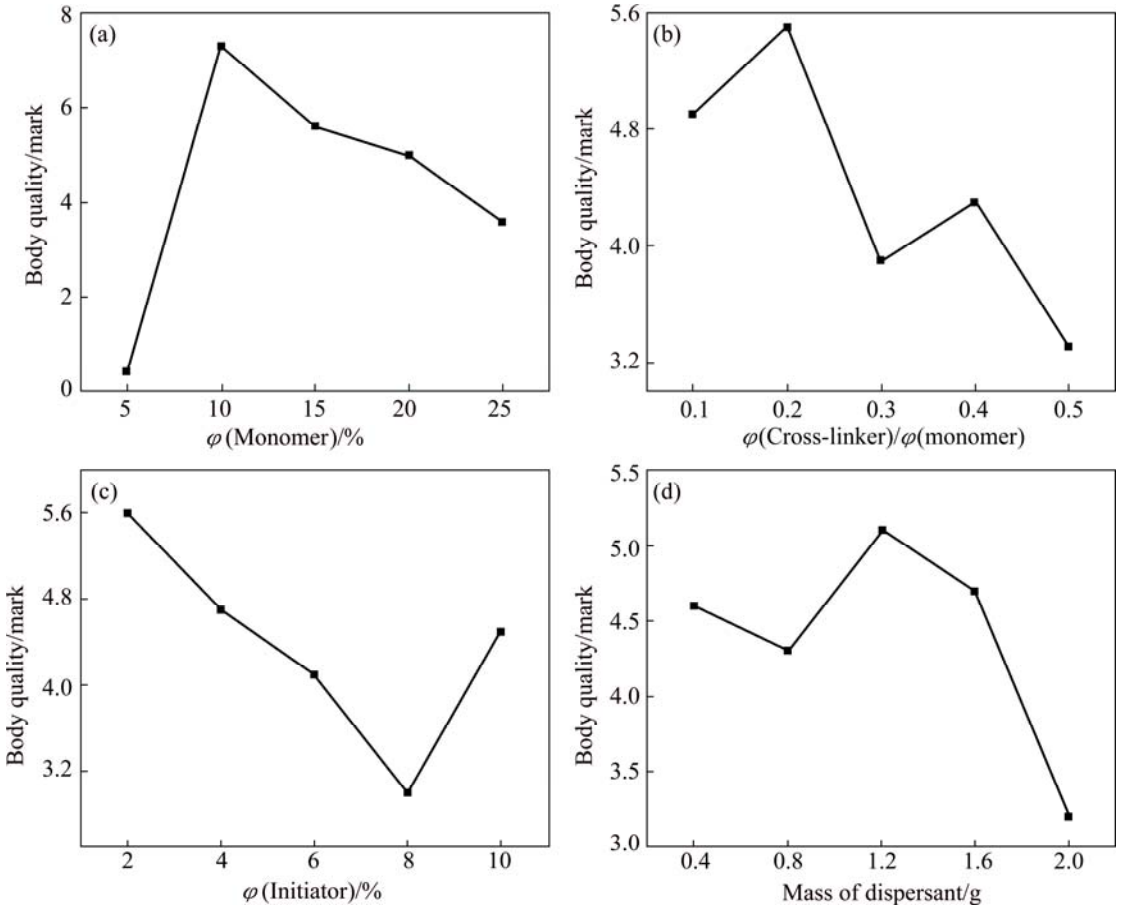

Fig. 3 Influence of process conditions on body quality: (a) Monomer content; (b) Cross-linker/monomer ratio; (c) Initiator content; (d) Mass of dispersant

Cross-linker plays the role in crosslinking and bridging the linear long-chain polymer molecules generated by radical polymerization monomer. The C═C bond of the cross-linker adheres to the long side of polymer chains to form a cross-linked and stable network structure by the bridge effect. As seen in Fig. 3(b), the optimum volume ratio of monomer to cross-linker is 0.2, in which the green body obtains good quality. The smaller ratios cause smaller "bridges" connecting the long chain and smaller polymerization degree of the polymer, therefore, lowering the strength of the green body. The green body is too soft to be easily deformed when demoulded and dried.

The polymerization degree improves with the increase of the ratio of cross-linker and monomer, but polymers still exhibit low cross-linked degree. The polymers have certain flexibility due to the large space between the chains in the solidifying stage, and this prevents non-uniform shrinkage and reduces inner stress in the forming stage. But when the ratio exceeds 0.2, the polymers have a high polymerization degree, multiple contraction centers in the body are formed, and the powder particles around polymer extend close connection, so polymer gel collapses very heavily in the drying stage, hindering solvent around the powder particles excluding [20].

Figure 3(c) shows that the quality of body decreases sharply with the increase of initiator. The increased initiator makes free radicals in the suspension uneven and excessive. When the polymerization of monomer completes, the molecular chain length is shortened and the integrity of polymer network is reduced. There may be other reaction inhibiting the polymerization of monomer and too many graft copolymers, leading to defects such as cracks in the body [15].

The formation of stable suspension depends on electrostatic interaction and steric hindrance of dispersant. As shown in Fig. 3(d), the optimum quality of green body can be achieved by the 1.2 g dispersant. This can be explained that when adding 0.4 or 0.8 g dispersants, the mixed metal powders subside heavily. Then, the suspension has separated layer that the suspension below has been solidified but the suspension with good fluidity on the surface forms the gel over a period of time, which is called asynchronous solidification. After drying at high temperature, the pure gel on the surface and the metal green body below have non-uniform shrinkage, then the gel on the surface has

cracks, and cracks extend further to the internal body. When adding 1.6 or 2.0 g dispersants, powder particles are bridged by excessive polymer chains, leading to non-uniform shrinkage and inner stress. Meanwhile, the surface spallation phenomenon in green bodies is not very clear, indicating that the dispersant plays very good surface spallation.

3.4 Mechanism analysis of cracks in different stages

In the forming stage, suspension cannot form the gel, the green body cannot be successfully demoulded, and the green body also has separated layer. These are mainly caused by the low content of organic monomers and low ratio of cross-linker to monomer. And the weak strength of the gel network impedes the formation of green body with enhanced strength. The height of the green body depends on the content of dispersants, sedimentation and coagulation occur if adding inappropriate content of dispersants. The results show that the inner stress in the green body can be minimized by adjusting the monomer and initiator contents and the volume ratio of cross-linker to monomers, and then the cracks could be reduced during forming and drying stages.

During drying process at low temperatures, green body exhibits multiple cracks due to the discordance of monomer as well as the volume ratio of monomer to cross-linker, as shown in Fig. 4. The inappropriate content of organic compounds makes the relative molecular mass, contraction centers and graft copolymers increase, then the inner stress in the green body develops, which possibly makes it an origin of cracks during subsequent treatment.

Fig. 4 Cracks of green bodies in process of low-temperature drying

During drying process at high temperatures, green body exhibits blowout cracks due to the removal of solvent, as shown in Fig. 5. The solvent diffuses and evaporates quickly at high temperatures, and cross-linked polymer gels, which are three-dimensional network structures, can swell and collapse reversibly when immersed in the solvents. The solvent is still not the continuous phase generated by the closed cavity, thus the solvent diffuses primarily through polymer gels around particles that is limited to exclusion, internal stress gradually increases over the pressure that body can stand, so blowout cracks appear [21]. Meanwhile, the blowout cracks set up on the surface, and extend to the interior, as shown in Fig. 5(b).

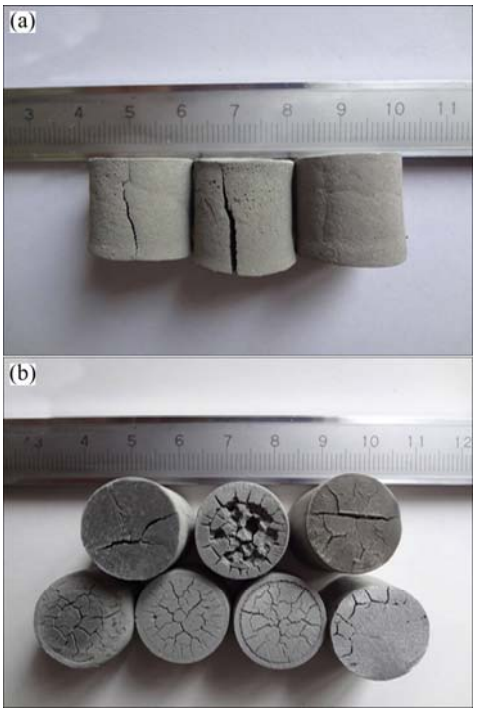

Fig. 5 Cracks of green bodies in process of high-temperature drying: (a) Cracks on surface; (b) Cracks on top and interior

Cracks and other defects do not appear in the burning out and sintering stages. The polymers can be removed clearly when burned out at slow heating rates, and the accumulation of inner stress can be inhibited when holding for enough time on the temperature of chemical bonds fracture. In the sintering stages, the alloy can be melted sufficiently and the sintering necks can be formed at the sintering temperature under suitable heating rate and holding time.

According to comprehensive analysis of results, the optimum gelcasting conditions for aluminum−copper alloy were 10% monomer, 2% cross-linker, 0.2% initiator, and 1.2 g dispersant, in which the prepared body exhibited the best quality.

4 Structure and property

Based on the optimal conditions, structure and property of the samples in the different stages are discussed. The fractures and surfaces of samples are shown in Fig. 6. It can be seen from Figs. 6(a) and (b) that the green bodies are actually composite materials composed of metal powders, solvent and organic polymer. When drying at 60 °C, the metal powders are wrapped by a large area of organic polymer. The composites have low strength and good flexibility, indicating that mechanical fracture cannot make the

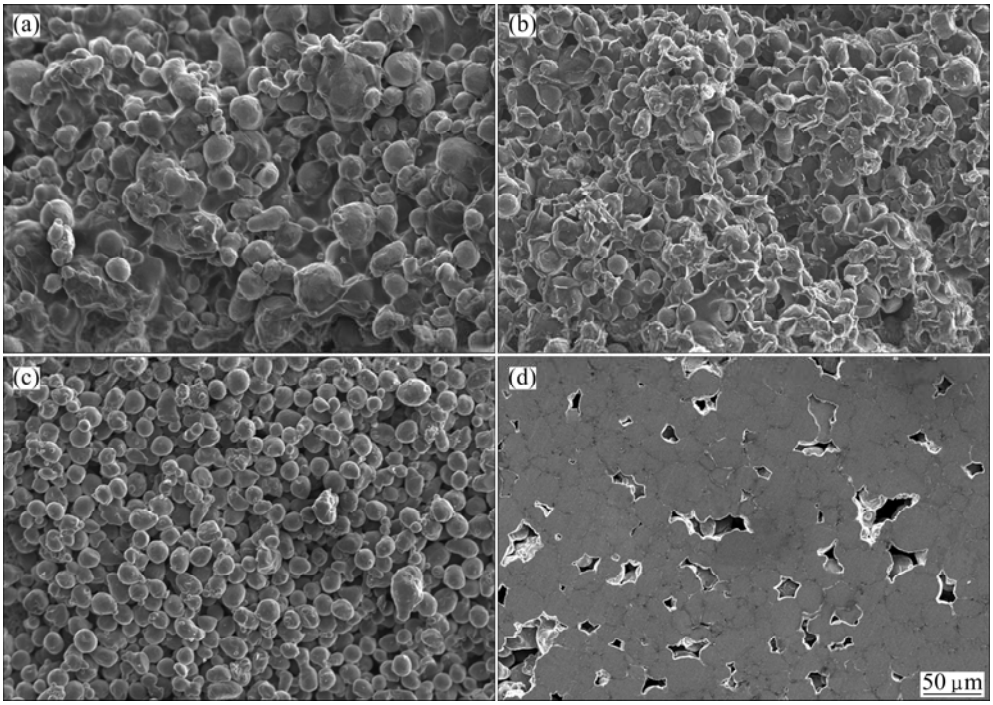

Fig. 6 Changes in fractures and surface morphology of Al−Cu samples dried at different temperatures: (a) 60 °C; (b) 170 °C; (c) 450 °C; (d) 670 °C

structure damage. When drying at 170 °C, the solvent evaporates, and the quantity of the pores increases obviously. Meanwhile, fracture appears in the network structures connecting powder particles, so the strength of the green body is determined by the strength of the network structures. In the degreasing stage, organic compounds are decomposed completely, and the powders are just connected mechanically (Fig. 6(c)). In the sintering stage, the polygonal pores appear on the surface of the sintered body after solvent and organic compounds volatile. The porous structure and interconnection between the pores and powders are clearly shown in the four stages. The formations of pores stem from the elimination of solvent and organic polymer.

Figure 7 shows that the aluminum−copper alloy and the sintering necks are formed in the internal pore. There are also interconnected pores between the particles. The pore size ranges from 5 to 50 μm surrounded by metal powders. From an XRD pattern (Fig. 8), the second phase of $AlCu_2$ is detected and desired mechanical properties are obtained.

Figure 9 shows the change of mass loss, transverse and longitudinal shrinkage in the drying, burning out and sintering stages. The mass loss in the drying stage is mainly attributed to the solvent elimination by diffusion towards the surface and evaporation as seen in Fig. 9(a). But the shrinkage is not obvious, because three-dimensional network does not change. Compared with the drying stage, organic compounds are decomposed into small molecules or gas, and three- dimensional network collapses, so shrinkage especially the longitudinal shrinkage increases greatly in the burning

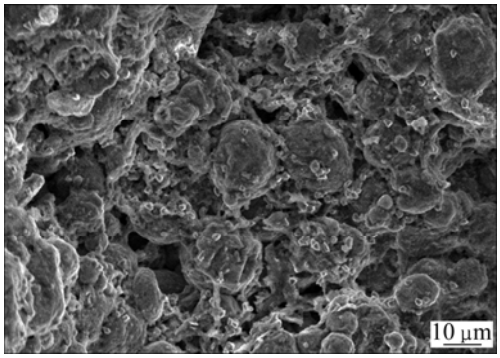

Fig. 7 Internal morphology of porous Al−Cu samples

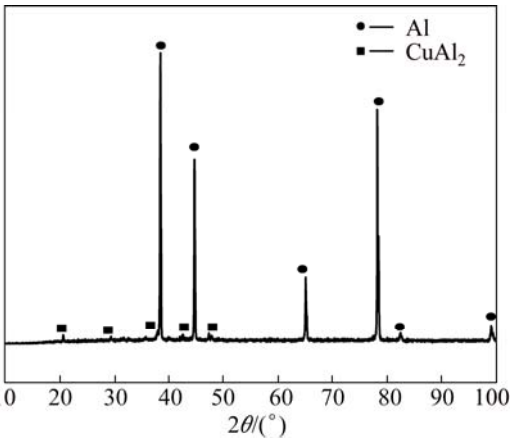

Fig. 8 X-ray diffraction pattern of Al−Cu samples

out stage, as shown in Fig. 9(b). During the sintering stage, there are small changes of mass, accompanied by the change of diameter and height as seen in Fig. 9(c). This is mainly because liquid phase appears during the sintering stage, and the sintering necks form between the metal particles.

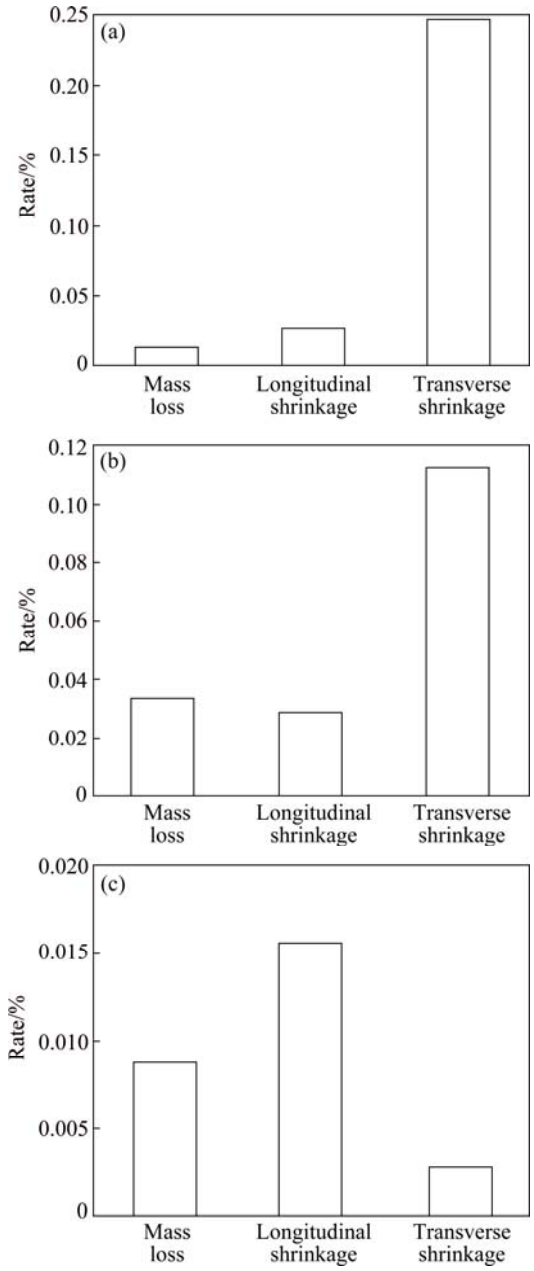

Fig. 9 Mass loss, transverse shrinkage and longitudinal shrinkage in drying (a), burning out (b) and sintering (c) stages

The density and property of the sintered body in mercury porosimetry are shown in Table 2. Without adding foaming agents, the porosity of sample can reach 38.78 %.

The cumulative pore volume and cumulative pore area curve data as the pore diameter in mercury porosimetry are shown in Fig. 10, and the median pore

Table 2 Density and porosity of sintered body

Bulk density/ ($g \cdot cm^{-3}$)	Skeletal density/ ($g \cdot cm^{-3}$)	Porosity/ %
1.61	2.63	38.78

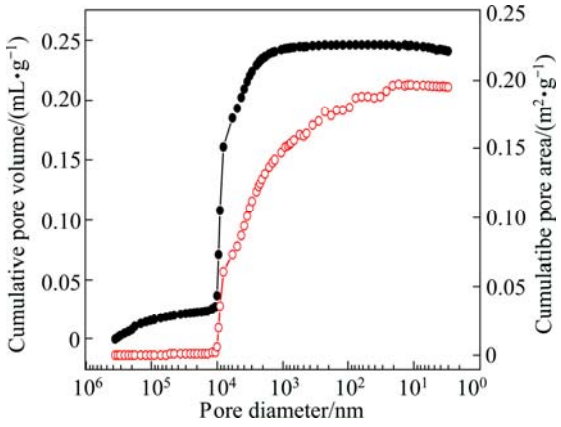

Fig. 10 Cumulative pore volume and cumulative pore area curves

diameter (volume and area) can be determined to be 8881.2 and 360718.6 nm, respectively. Both curves exhibit plateaus at small pores. It can be seen that intrusion volume up to 0.2463 mL/g leads to the completeness of pore-filling. This clearly indicates that the onset of mercury intrusion appears over the range of pore diameter 7.2−13.7 nm.

The pore size distribution exhibits a hierarchical pore structure with a sharp and broad peaks centered at 1300−5860 and 5860−10700 nm, respectively, as shown Fig. 11. The contribution of the dominant pore diameter to pore volume was located between 5860−10700 nm, with around 76.82% of volume contribution, as shown in Fig. 10. The “double hump distribution” makes the pore size center on the mesopore and micro pore.

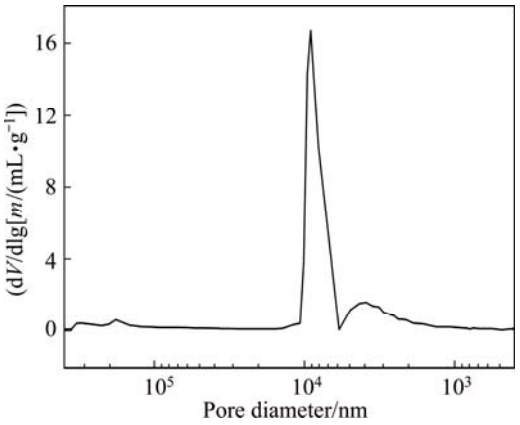

Fig. 11 Pore size distribution

5 Conclusions

1) In the forming stage, suspension cannot form the gel, the green body cannot be successfully demoulded

and also has separated layer due to the low contents of solidification agents and dispersant.

2) Green body exhibits multiple cracks in the low temperature drying process, but shows blowout cracks in the high temperature drying process.

3) The optimum gelcasting conditions are 10% monomer, 2% cross-linker, 0.2% initiator, and 1.2 g dispersant, in which the prepared body exhibits the best quality.

4) The mechanism of process condition in eliminating the cracks and forming the pores in the five stages is also analyzed.

5) Without adding foaming agents，the opening porosity of sample reaches 38.78% with pore diameter ranging from 10 to 10000 nm.

References

[1] GUO Hong-min, ZHANG Ai-sheng, YANG Xiang-jie, YAN Ming-ming. Grain refinement of Al−5% Cu aluminum alloy under mechanical vibration using meltable vibrating probe [J]. Transactions of Nonferrous Metals Society of China, 2014, 24(8): 2489−2496.

[2] PINTO M A, CHEUNG N, IERARDI M C F, GARCIA A. Microstructural and hardness investigation of an aluminum–copper alloy processed by laser surface melting [J]. Materials Characterization, 2003, 50: 249−253.

[3] ZHANG Ming, ZHANG Wei-wen, ZHAO Hai-dong, ZHANG Da-tong, LI Yuan-yuan. Effect of pressure on microstructures and mechanical properties of Al−Cu-based alloy prepared by squeeze casting [J]. Transactions of Nonferrous Metals Society of China, 2007, 17(3): 496−501.

[4] YOUNG K P, KERKWOOD D H. The dendrite arm spacings of aluminum-copper alloys solidified under steady-state conditions [J]. Metallurgical Transactions A, 1975, 6: 197−205.

[5] WANG Hai-long, ZHANG Rui, HU Xing, WANG Chang-An, HUANG Yong. Characterization of a powder metallurgy SiC/Cu−Al composite [J]. Journal of Materials Processing Technology, 2008, 197: 43−48.

[6] GILISSEN R, ERAUW J P, SMOLDERS A, VANSWIJGENHOVEN E, LUYTEN J. Gelcasting, a near net shape technique [J]. Materials and Design, 2000, 21: 251−257.

[7] STAMPFL J, LIU H, NAM SW, SAKAMOTO K, TSURU H, KANG S, COOPER AG, NICKE A, PRINZ F B. Rapid prototyping and manufacturing by gelcasting of metallic and ceramic slurries [J]. Materials Science and Engineering A, 2002, 334: 187−192.

[8] JIA Cheng-chang, BEKOUCHE K, YUAN Hai-ying, ZHANG Xiu-li, SHI Yan-tao, LIU Wei-hua. Non-water-based gelcasting of metal powders [J]. Powder Metallurgy Technology, 2013, 31: 223−228. (in Chinese)

[9] SEPULVEDA P, BINNER J G P. Evaluation of the in situ polymerization kinetics for the gelcasting of ceramic foams [J]. Chemistry Materials, 2001, 13: 3882−3887.

[10] LOCS J, ZALITE V, BERZINA-CIMDINA L, SOKOLOVA M. Ammonium hydrogen carbonate provided viscous slurry foaming—A novel technology for the preparation of porous ceramics [J]. Journal of the European Ceramic Society, 2013, 33: 3437−3443.

[11] SUN Yan-rong, HUANG Yong, YANG Jin-long, MA Li-rong. Research progress in improvement of gel system for gelcasting based on defects's controlling [J]. Materials Review 2010, 24(2): 80−83. (in Chinese)

[12] YANG Jin-long, YU Juan-li, HUANG Yong. Recent developments in gelcasting of ceramics [J]. Journal of the European Ceramic Society, 2011, 31: 2569−2591.

[13] MORAES R R, GARCIA J W, BARROS M D, LEWIS S H, PFEIFER C S, LIU J, STANSBURY J W. Control of polymerization shrinkage and stress in nanogel-modified monomer and composite materials [J]. Dental Materials, 2011, 27: 509−519.

[14] BARATI A, KOKABI M, FAMILI M H N. Drying of gelcast ceramic parts via the liquid desiccant method [J]. Journal of the European Ceramic Society, 2003, 23: 2265−2272.

[15] HUANG Yong, ZHANG Li-ming, YANG Jin-long, XIE Zhi-peng, WANG Chang-an, CHEN Rui-feng. Research progress of new colloidal forming processes for advanced ceramics [J]. Journal of the Chinese Ceramic Society, 2007, 35: 129−136.

[16] XIAO Chun-xia, GAO Lei, LU Ming-jing, CHEN Han, GUO Lu-cun. Effect of polyvinylpyrrolidone on rheology of aqueous SiC suspensions with polyethylene glycol as binder [J]. Colloids and Surfaces A: Physicochemical and Engineering Aspects, 2010, 368: 53−57.

[17] TONG Jian-feng, CHEN Da-ming. Preparation of alumina by aqueous gelcasting [J]. Ceramics International, 2004, 30: 2061−2066.

[18] HUANG Yong, YANG Jin-long. Novel colloidal forming of ceramics [M]. Heidelberg Berlin: Springer, 2010.

[19] CHEN Da-ming. Gel casting technology and application of advanced ceramic materials [M]. Beijing: National Defense Industry Press, 2011. (in Chinese)

[20] ORTEGA F S, SEPULVEDA P, PANDOLFELLI V C. Monomer systems for the gelcasting of foams [J]. Journal of the Chinese Ceramic Society, 2002, 22: 1395−1401.

[21] LIU Xiao-guang, LI Guo-jun, TONG Jian-feng, CHEN Da-ming. Study on stability of zirconia aqueous slurries [J]. Journal of Materials Engineering, 2003: 30−32. (in Chinese)

凝胶注模工艺参数对多孔铝铜合金品质的影响

袁海英，贾成厂，王聪聪，常宇宏，张新新，Bekouche KARIMA，王召利

北京科技大学 材料科学与工程学院，北京 100083

摘　要：通过凝胶注模工艺制备多孔铝铜合金。研究凝胶注模工艺参数如单体含量、交联剂与单体的比例、分散剂和引发体系 4 个因素对坯体高度、固化时间和坯体品质 3 个指标的影响。其中分散剂对坯体高度，单体对坯体质量的影响最大。通过分析得出最佳工艺为：单体体积分数 10%、交联剂体积分数 2%、引发剂体积分数 0.2%、分散剂质量 1.2 g，在此条件下坯体呈现最好的品质。同时探讨工艺参数消除裂纹和形成孔结构的机理。利用压汞法得出孔直径在 10~10000 nm 范围内，开孔气孔率达到 38.78 %。

关键词：多孔 Al−Cu 合金；非水基凝胶注模；工艺参数；裂纹；气孔

(Edited by Yun-bin HE)